

Microgram BaCl₂ Ablation Targets for Trapped Ion Experiments

Noah Greenberg,^{1, a)} Akbar Jahangiri Jozani,¹ Collin J. C. Epstein,¹ Xinghe Tan,¹ Rajibul Islam,¹ and Crystal Senko¹

Institute for Quantum Computing and Department of Physics and Astronomy, University of Waterloo, Waterloo, Ontario N2L 3G1, Canada

(Dated: 13 February 2024)

Trapped ions for quantum information processing has been an area of intense study due to the extraordinarily high fidelity operations that have been reported experimentally. Specifically, barium trapped ions have been shown to have exceptional state-preparation and measurement (SPAM) fidelities. The $^{133}\text{Ba}^+$ ($I = 1/2$) isotope in particular is a promising candidate for large-scale quantum computing experiments. However, a major pitfall with this isotope is that it is radioactive and is thus generally used in microgram quantities to satisfy safety regulations. We describe a new method for creating microgram barium chloride (BaCl₂) ablation targets for use in trapped ion experiments and compare our procedure to previous methods. We outline two recipes for fabrication of ablation targets that increase the production of neutral atoms for isotope-selective loading of barium ions. We show that heat-treatment of the ablation targets greatly increases the consistency at which neutral atoms can be produced and we characterize the uniformity of these targets using trap-independent techniques such as energy dispersive x-ray spectroscopy (EDS) and neutral fluorescence collection. Our comparison between fabrication techniques and demonstration of consistent neutral fluorescence paves a path towards reliable loading of $^{133}\text{Ba}^+$ in surface traps and opens opportunities for scalable quantum computing with this isotope.

I. INTRODUCTION

Ion trapping is a leading platform for quantum simulation and quantum computing due to its scalability^{1,2}, high-fidelity entangling gates^{3,4}, and long coherence times⁵. A leading trapped ion species that has recently emerged due to its unrivaled state-preparation and measurement fidelities is barium, specifically the $^{137}\text{Ba}^+$ and $^{133}\text{Ba}^+$ isotopes⁶⁻⁸. Barium has many attractive atomic features such as visible wavelength transitions for easier optical engineering⁹ and a metastable state for shelving^{10,11}.

The caveats to the ^{133}Ba isotope are that it is typically sourced as a synthetic radioactive salt, either as BaCl₂ or Ba(NO₃)₂, and can only be used in quantities deemed safe by a governing regulatory body. For example, the Canadian Nuclear Safety Commission (CNSC) dictates that holders of a Basic Level license can work with up to ~ 55.5 MBq of the ^{133}Ba isotope¹². In this manuscript, we aim to create a recipe for the fabrication of reliable microgram quantity atomic sources for trapped ion experiments in order to simplify regulatory requirements, reduce worker exposure, and increase the duration that a worker can safely be near the radioactive source. We choose to work with BaCl₂ over Ba(NO₃)₂ since BaCl₂ has been used to previously trap the ^{133}Ba isotope⁷.

Loading an ion trap reliably with microgram quantities of any isotope is difficult and so far $^{133}\text{Ba}^+$ trapping has only been reported by a sole academic group¹³, despite there being significant interest from the research community¹⁴⁻¹⁷. We present the first systematic study of microgram BaCl₂ ablation targets for use in trapped ion experiments and fabricate targets that produce consistent and reliable neutral fluorescence¹⁸. The longevity of the fabricated ablation targets as well as the

consistency at which the targets produce measurable neutral fluorescence is investigated. Given that none of the properties we investigate are isotope-dependent, we use ^{138}Ba as a proxy for ^{133}Ba because ^{138}Ba is naturally abundant and nonradioactive.

A major hurdle preventing consistent neutral barium production from microgram BaCl₂ ablation targets are the concentrated BaCl₂ ‘rings’ that form during the deposition process, pictured in Fig. 1a. The ‘coffee ring effect’ is a well studied phenomena¹⁹⁻²¹ and we remedy this issue through the heat-treatment of microgram BaCl₂ ablation targets.

We present two recipes for creating these targets, both of which use a form of heat-treatment to either melt the salt on the surface of the substrate or melt the underlying metallic substrate. The first recipe resistively heats a strip of platinum to the melting point of BaCl₂ ($\sim 960^\circ\text{C}$), melting the salt on the surface¹³. The second recipe is a novel process in which BaCl₂ is combined with aluminum and heated in a vacuum chamber. In this manuscript, we test these two types of heat-treated targets, hereafter referred to as the Pt* and Al* ablation targets, and compare this with a Pt ablation target that has not been heat-treated. The ablation targets are pictured in the appendix.

After heat-treatment, we map the distribution of BaCl₂ over the ablation target surfaces and yield of ablated ^{138}Ba using techniques that are independent of the details of any specific ion trap, such as energy dispersive X-ray spectroscopy (EDS) and fluorescence-based detection.

We find that the uniformity of the ablation targets after heat-treatment is enhanced. Neutral fluorescence is detected from both non heat-treated and heat-treated microgram BaCl₂ ablation targets, indicating their viability in trapped ion experiments. However, the consistency at which ^{138}Ba atoms can be detected from the heat-treated targets exceeds that of ablation targets that have not undergone heat-treatment. We show that heat-treated ablation targets are at least four times as likely to produce detectable amount of neutral ^{138}Ba atoms

^{a)}n2greenb@uwaterloo.ca

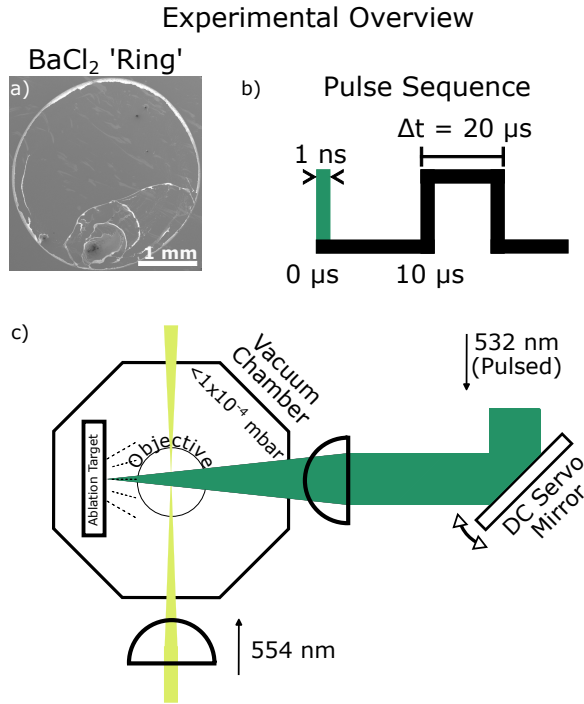


FIG. 1: a) A ring of BaCl₂ containing ~ 1 -2 μg of material deposited on a gold microfabricated substrate. The microfabricated gold substrate is not an ablation target, but simply a smooth surface to estimate the amount of deposited BaCl₂. b) Pulse sequence of the experiment for collecting neutral fluorescence. The ablation pulse seen on the photo-multiplier tube (PMT) signals the start of the experiment, and the majority of the neutral atoms arrive roughly 10 μs later¹⁴. The photon collection window is from 10-30 μs relative to the start of the experiment. c) Top-down view of the vacuum and optical system used to collect neutral fluorescence from the atomic plume after ablation of targets. An objective and PMT sit below the ablation testing chamber.

and that neutral production can be sustained for at least three times as many ablation pulses while still producing measurable amounts of neutral fluorescence.

II. DEPOSITION OF BaCl₂

The first step in fabricating any microgram quantity BaCl₂ ablation target is to deposit the salt onto a substrate. Radioactive ¹³³Ba salt can be purchased from suppliers such as the Eckert & Ziegler Group and comes dissociated in a vial of solvent. A buyer can choose the given amount of radioactivity in a vial, but for calculation purposes we assume the vial has ~ 37 MBq of radioactivity in order to avoid being near the CNSC ~ 55 MBq radiation limit. Since the deposition presented here is meant to be compatible with the deposition of radioactive BaCl₂, we create similar solutions with naturally abundant BaCl₂ from Sigma-Aldrich (342920-10G) and deionized water. The procedure used to create these ablation

targets is the same procedure is used for both the Pt* and Pt filament-like targets as well as the Al* targets.

The amount of ¹³³Ba salt in a 37 MBq solution can be calculated from the half-life $t_{1/2}$ of the radioactive substance, the activity A , the reaction rate constant λ , and Avogadro's number N_a ²²:

$$t_{1/2} = \frac{\ln(2)}{\lambda}, \quad (1)$$

$$A = \lambda N_a n. \quad (2)$$

The value of the known parameters $t_{1/2} \approx 3.33 \times 10^8$ s, $A = 3.7 \times 10^7$ Bq, and $N_a \approx 6.022 \times 10^{23}$ mol⁻¹ can be used to find the number of moles n of ¹³³Ba. Given the molar mass of radioactive BaCl₂ is ~ 203.8 g/mol²³, we calculate that there is ~ 6 μg of BaCl₂ in a radioactive vial with the given parameters. We test targets with ~ 5 μg of nonradioactive BaCl₂.

A. Deposition Preparation & Process

The substrate, whether it is a Pt*, Pt, or an Al* target is cleaned following typical ultra-high vacuum protocol. The platinum is purchased from Sigma-Aldrich (327433) and the targets are cut into strips roughly 20 x 2.5 x 0.125 mm. The aluminum targets are made with 5-10 mg of aluminum foil from Kurt J. Lesker (FOILA24) melted onto a machined titanium holder. We sonicate the pieces in Sparkleen™, rinse with deionized water, and sonicate again with acetone.

A 1-liter solution of deionized water is prepared with 20 mg of BaCl₂. The BaCl₂ is weighed on a digital scale with 1 mg precision and added to the beaker of deionized water. This is stirred until no more visible salt crystals are present and it has completely dissociated, usually within five minutes.

We employ a 10-100 μL PuroPET variable volume micropipette with 10 μL disposable pipette tips to deposit 10 μL of solution at a time. We deposit 25 drops to ensure that ~ 5 μg of salt is deposited. One drop of solution is applied to the substrate at a time until the desired amount of BaCl₂ has been applied.

A hot plate is then set to 115° C to increase the evaporation rate of the solvent. At this temperature, we find 10 μL drops will not boil but evaporate at an increased rate. The evaporation of a 10 μL drop takes about a minute. If the temperature set point is higher, the solution begins to boil vigorously, splattering BaCl₂ and causing contamination and material loss.

III. HEAT-TREATMENT OF BaCl₂ TARGETS

A. Resistive Heating of Pt*

After the deposition is complete, the ablation target is attached with alligator clips to a Chroma 62012P-80-60 programmable direct-current source and resistively heated by

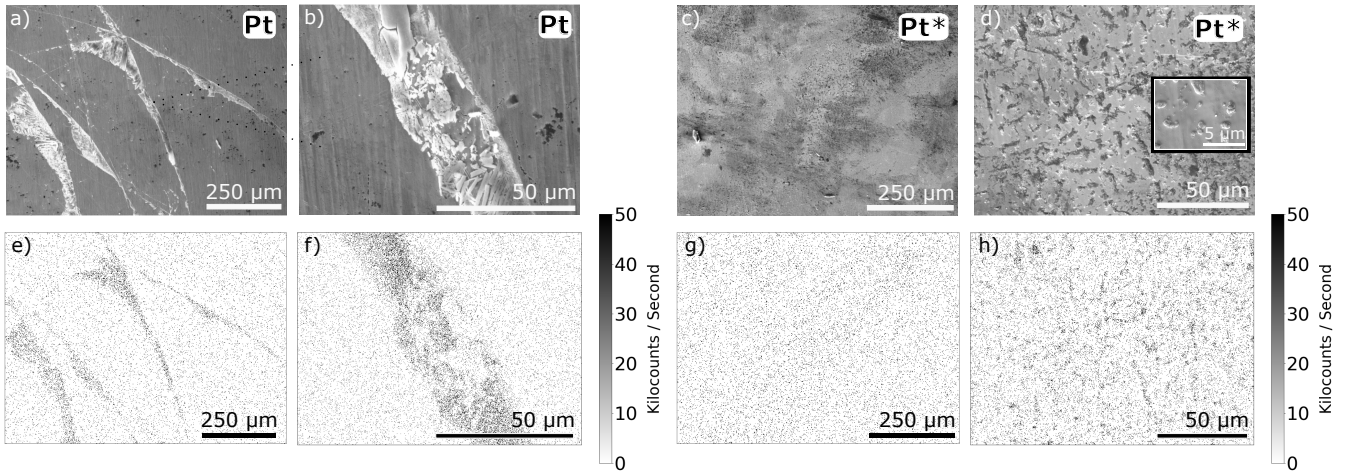


FIG. 2: a-d) SEM images of BaCl₂ deposited onto platinum substrates near the center of the ablation targets. The BaCl₂ of the Pt targets are concentrated into relatively thick rings, while the heat-treated Pt* ablation targets have BaCl₂ uniformly spread over the entire surface in micron size crystals. e-h) Corresponding energy dispersive x-ray spectroscopy (EDS) maps of the above SEM images verifying the presence of barium after the deposition of BaCl₂ and heat-treatment of the Pt* ablation targets. All counts measured using EDS correspond to the barium $L_{\alpha 1}$ line centered at 4.46 KeV. The Al* ablation targets are not mapped with EDS as the surface is quite rough and the underlying substrate (below the aluminum layer) is titanium with a $K_{\alpha 1}$ line at 4.51 KeV, which is difficult to distinguish from barium.

running a large amount of current $I \approx 55$ A through the target until the center of the filament glows bright orange and reaches temperatures $> 960^\circ$ C. This process is typically sustained for 10-20 seconds.

B. High Vacuum Heating of Al*

The second method of heat-treatment utilizes a high-vacuum BORALECTRIC® heating stage from Tectra GmbH, capable of reaching 1200° C. The chamber is evacuated with a turbo-molecular pump until the pressure reaches $\leq 1 \times 10^{-4}$ mbar to prevent oxidation of the target and heating stage.

The heating stage is ramped to the desired temperature of 760° C. At this temperature a few milligrams of aluminum foil (MP = 660° C) will melt within a couple of minutes once the machined target has come to equilibrium with the heating stage. The sample is visible through a viewport and the heat shield, so the phase transition can be visually confirmed. After the aluminum has melted, the stage is switched off and allowed to return $< 100^\circ$ C before venting and retrieving the samples. Once this first heat-treatment has occurred, BaCl₂ is deposited on the surface of the Al target and the aluminum along with the BaCl₂ is again heated to $\sim 760^\circ$ C in vacuum in order to diffuse the salt. The aluminum is initially melted without BaCl₂ in order to create a mechanically stable surface for depositing the salt.

IV. MEASUREMENT TECHNIQUES

A. EDS Measurements of BaCl₂ Targets

Commonly used in conjunction with a scanning electron microscope, EDS is a technique for probing the elemental composition on a sample surface²⁴. Using EDS after sample fabrication allows us to confirm the presence of BaCl₂ on the surface of the Pt and Pt* targets and quantify the uniformity before ablation as shown in Fig. 2. The Pt targets depicted in Fig. 2a-b and Fig. 2e-f show concentrated areas of BaCl₂. While the heat-treated Pt* targets in Fig. 2c-d and Fig. 2g-h show that the surface distribution of BaCl₂ is relatively uniform. We also map areas (not depicted) that are 100-150 μm in length. We find that the sampled spots on the Pt* targets typically have ~ 1 -3% barium by weight on the surface before laser ablation, with an average of 2.5% and a coefficient of variation of 0.58. A total of 53 spots were sampled on the Pt* target.

B. Collection of Neutral Fluorescence from ¹³⁸Ba Atoms

We evaluate the Pt, Pt*, and Al* targets by collecting neutral fluorescence after ablation on a photo-multiplier tube (PMT), which can be correlated to the probability of loading¹⁴. The pulse sequence used for collecting fluorescence is depicted in Fig. 1b. The ablation target is mounted 12 mm from the center of the chamber. There are two beams entering the chamber, one to drive the resonant $6s^2\ ^1S_0 \leftrightarrow 6s6p\ ^1P_1$ transition at 554 nm and a perpendicular 532 nm Nd:YAG nanosecond pulsed solid-state laser from RPMC

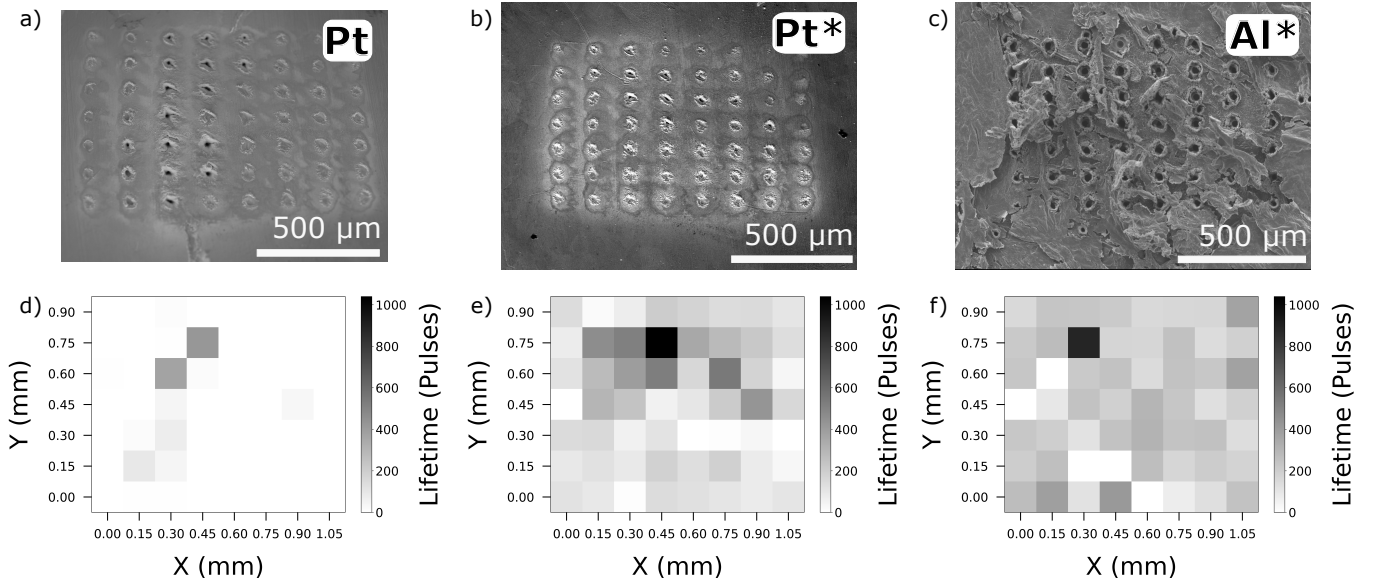


FIG. 3: a) Scanning electron microscope (SEM) picture of 56 ablation spots on a Pt ablation target that has not been heat-treated. On this sample, 17 / 56 ablation spots produced measurable neutral fluorescence meeting the σ_1 criteria outlined in Section V. This is the best performing Pt target, with the other three Pt targets producing significantly fewer neutral atoms, despite ablating similar BaCl₂ rings. b) SEM image of a heat-treated Pt* ablation target with 55 / 56 spots producing enough neutral atoms to meet the σ_1 criteria. c) SEM image of a heat-treated Al* ablation target with 51 / 56 spots producing enough neutral atoms to meet the σ_1 criteria. d-f) Heatmaps of the ablation spot lifetime (number of pulses) corresponding to the above SEM images. Each ablated spot is spaced by $\sim 150 \mu\text{m}$, which is roughly the beam waist of the laser focal point on the ablation target.

Lasers Inc. (WEDGE-HB 532) for ablation of the BaCl₂. The 554 nm beam is aligned orthogonal to the normal of surface of the target to reduce Doppler broadening. After each ablation pulse ($\sim 0.42 \pm 0.02 \text{ J/cm}^2$ pulse fluence), counts are detected on a PMT from Hamamatsu (H10682-210) through a home-built 1" diameter objective (NA = 0.26, WD = 43 mm). The beam orientation and experimental setup is depicted in Fig. 1c. We consider only single-shot experiments, where only one ablation pulse is used to generate a cloud of neutral atoms. The ablation vacuum chamber from Kimball Physics (53-180000) is identical to the part used in previous ablation experiments involving a four-rod trap, as is the aforementioned objective¹⁴.

In order to discern counts from ¹³⁸Ba atoms and counts from background events, we set the resonant frequency for driving the $6s^2 \ ^1S_0 \leftrightarrow 6s6p \ ^1P_1$ transition to 541.433000 THz and tune the 554 nm laser 1 GHz off-resonance to 541.432000 THz every other pulse. The frequency of the 554 nm laser is stabilized via a HighFinesse WS8-2 wavemeter. Neutral fluorescence is collected 10 μs after ablating the center of the target and the collection window lasts for 20 μs .

V. RESULTS

We ablate targets prepared with 5 μg of BaCl₂ and search for neutral fluorescence produced from the ablation targets as a means to gauge the viability of the targets for use in trapped ion experiments. Both consistency and longevity of spots on

the ablation targets are compared across the three target types as shown in Fig. 3. The average spot lifetime of the Pt target shown in Fig. 3d is ~ 69 pulses, compared with ~ 185 and ~ 232 pulses for the Pt* and Al* targets depicted in Fig. 3e and Fig. 3f, respectively.

The lifetime of an ablation spot is evaluated based on a running average of the counts collected shortly after the last 50 ablation pulses. In this case, 25 pulses are when the 554 nm laser frequency is on-resonance and 25 pulses are when the frequency is tuned off-resonance. All ablation spots are evaluated for a minimum of 50 pulses. If the average of the counts on-resonance c_R falls within one standard deviation σ_1 or two standard deviations σ_2 of the off-resonance c_O count average, the spot is considered ‘dead’ and unlikely to produce detectable ¹³⁸Ba atoms. The lifetime of an ablation spot can be evaluated using either the σ_1 or σ_2 criteria. A spot is considered ‘dead’ spot if it satisfies Eq. 3.

$$c_R \leq c_O + \sigma_n \quad (3)$$

Over the course of an experiment, the standard deviation of the 554 nm laser frequency is $< 2 \text{ MHz}$ shot-to-shot. The saturation parameter is set to $s > 100$ for the $6s^2 \ ^1S_0 \leftrightarrow 6s6p \ ^1P_1$ transition when collecting neutral fluorescence to ensure sufficient power.

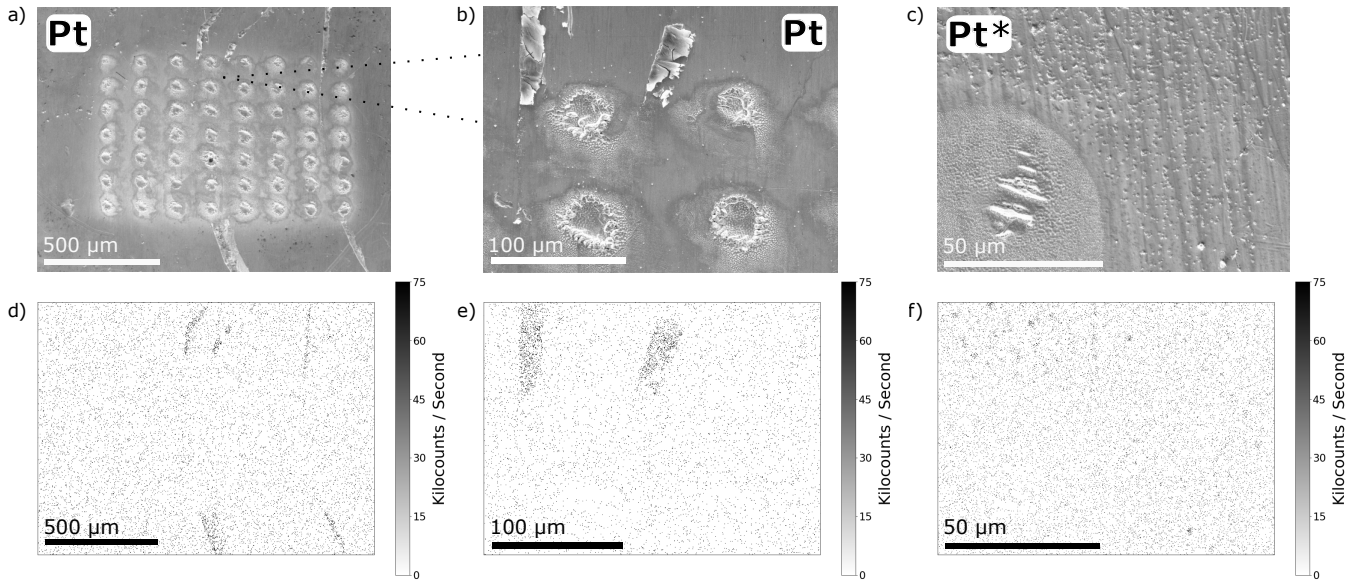


FIG. 4: a) A grid of 56 ablation spots covering $\sim 1.26 \text{ mm}^2$ on a Pt ablation target. Only $\sim 1 / 12$ ablation spots aligned directly onto the BaCl₂ ring satisfied the σ_1 criteria. b) SEM image of BaCl₂ rings that have been removed from the surface due to ablation without resulting in detection of neutral atoms. c) SEM image of an ablated spot on a Pt* target. An ablation spot on the left side of the image has removed the $\sim 1 \mu\text{m}$ BaCl₂ crystals, but BaCl₂ is still evident outside of the ablation spot. The surface of the ablated spot is rough and appears similar to BaCl₂ crystals, but it is devoid of any material except the platinum substrate. d-f) Corresponding EDS mappings of the ablated regions in SEM images shown in a-c), confirming the removal of the BaCl₂ after ablation.

Target	c_1 (Pulses)	Yield (σ_1 Criteria)	c_2 (Pulses)	Yield (σ_2 Criteria)
Pt	36	43 / 79 [†] ≈ 0.54	32	10 / 79 ≈ 0.13
Pt*	158	142 / 168 ≈ 0.85	91	95 / 168 ≈ 0.57
Al*	184	134 / 175 ≈ 0.77	123	93 / 175 ≈ 0.53

†: Only 79 / 448 total spots on the Pt type targets hit a BaCl₂ ring, so only these ablation spots are considered in the average lifetime calculations. In realistic scenarios, it is not possible to deterministically hit the ring, so the practical yield is 43 / 448 ≈ 0.10 .

TABLE I: Mean lifetime c_1 of all ablation spots on each target that satisfies the σ_1 criteria in Section V. Given that the heat-treated Pt* and Al* ablation targets have a significantly more uniform distribution of BaCl₂ on the surface, all spots on these target types were considered in the average lifetime calculations. Mean lifetime c_2 of only the spots that produced significant neutral fluorescence as defined by the σ_2 criteria. The fraction of tested ablation spots that meet the σ_1 and σ_2 criteria are also listed for each ablation target type.

A total of ten ablation targets were tested: three targets for each of the heat-treated Pt* and Al* type targets and four of the Pt type target, listed in Table I. A minimum of 56 spots were collected from each of the ten targets. The heat-treated Pt* and Al* targets performed significantly better in both consistency and ¹³⁸Ba production on average when compared with the Pt targets that have not undergone heat-treatment. We

find that despite ablating directly on the BaCl₂ ‘rings’ of the Pt targets, often there is no discernible neutral fluorescence collected above the background. We confirm with SEM and EDS measurements that BaCl₂ is removed from the surface of the Pt and Pt* targets at ablated spots, as depicted in Fig. 4, but only a single spot from the Pt target shown in Fig. 4 yielded measurable neutral counts.

VI. CONCLUSION

We have outlined and tested two heat-treatment techniques for fabricating microgram quantity BaCl₂ ablation targets to be used in isotope-selective loading of barium ions, motivated by trapping efforts aimed at the ¹³³Ba⁺ isotope. With both heat-treatment techniques, a more uniform distribution of the BaCl₂ was created on the surface of the substrate, creating targets that are at least four times more likely to produce neutral atoms. The total yield of ablated barium atoms is also significantly higher with ablation spot lifetimes three to five times higher for heat-treated targets. Similarly, when testing ablation targets with $> 100 \mu\text{g}$ of BaCl₂, the uniformity of the salt on the surface is improved after heat-treatment. More details on the uniformity of the $> 100 \mu\text{g}$ targets, as well as observations on contamination of nearby surfaces by ablated BaCl₂ can be found in the appendices.

We find that in the case of the platinum substrate ablation targets, consistent production of neutral fluorescence is increased significantly when the substrate is heated to tem-

peratures that enable melting of the microgram quantities of BaCl₂. This is due to the fact that, when melted, concentrated rings of BaCl₂ that form during the deposition process are dispersed over the substrate surface. Given the spatial uniformity of the BaCl₂ on the surface of the Pt* ablation targets and the ease of preparation compared with the Al* targets, we find that of the tested approaches the Pt* target performs with the best consistency. Our presented recipe and results enable a more consistent preparation of BaCl₂ ablation targets, paving the way for integration of the ¹³³Ba⁺ isotope into scalable quantum information experiments. Due to the inherent advantages ¹³³Ba⁺ offers for quantum information processing, our research removes a major obstacle toward advancing trapped ion quantum computing technology.

ACKNOWLEDGMENTS

This research was supported in part by the University of Waterloo, Canada First Research Excellence Fund (CFREF), Grant No. CFREF-2015-00011, and the Ontario Early Researcher Award. CS is also supported by a Canada Research Chair.

We thank Zachary J. Wall and Samuel R. Vizvary, as well as the other group members at the University of California-Los Angeles for stimulating discussion and transparency involving their successful loading of ¹³³Ba⁺.

Appendix A: Procurement of ¹³³Ba

The ¹³³Ba isotope can be purchased from Eckert & Ziegler, Oak Ridge National Lab, or NIST. For future experiments, we have purchased ¹³³Ba from Eckert & Ziegler with "no stable carrier added" and request that the sample be pulled from the master batch with the highest "specific radioactivity".

Appendix B: Aluminum Heat-Treatment & Ablation Targets

We present a figure showing targets that were ablated during the experiment as well as a rendering of the high-vacuum chamber and heating stage that was used to manufacture the Al* ablation targets.

Appendix C: Trap Contamination from BaCl₂ Ablation Targets

Ablation of a non heat-treated natural abundance BaCl₂ targets was also conducted in an ultra-high vacuum chamber ($\sim 4.4 \times 10^{-11}$ mbar) where a surface trap²⁵ was installed ~ 15 mm away from a macroscopic BaCl₂ target containing ~ 40 mg worth of salt. The surface trap is a defected test trap with many electrodes shorted to ground. We collected neutral fluorescence from ¹³⁸Ba as we ablated the target. After confirming the presence of ¹³⁸Ba at the trapping region, the physical test trap was removed and imaged using an SEM.

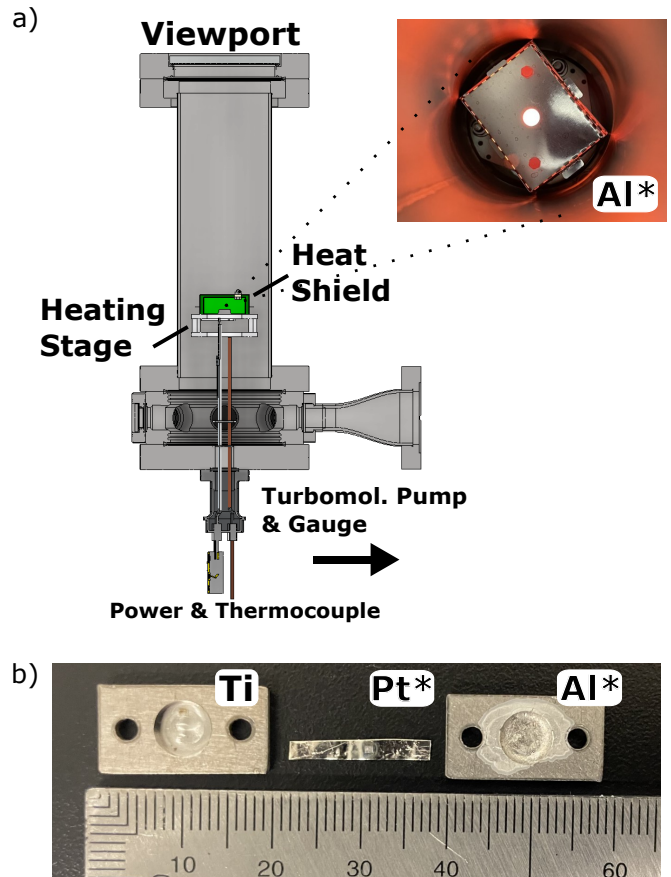


FIG. 5: a) Cross-sectional view of the high-vacuum heating stage used to create Al* ablation targets with microgram quantities of BaCl₂. b) Tested ablation targets with $\sim 5 \mu\text{g}$ of BaCl₂ on the surface. The appearance of the heat-treated Pt* and Pt targets are similar. The ruler depicted is in millimeters.

Significant trap contamination was found, visible on SEM images after ablation of macroscopic BaCl₂ targets, as shown in Fig. 6. BaCl₂ is a dielectric, so the chances of it directly shorting electrodes is unlikely. However, excess material deposited on the surface of microfabricated traps can exacerbate anomalous heating of the trapped ion motion. This is an area of considerable focus^{26,27} and a limiting factor in making even smaller micro-fabricated surface traps²⁸.

Appendix D: Heat-Treated Macroscopic Targets

We test heat-treated platinum targets with macroscopic (visible) varying amounts of BaCl₂ in order to evaluate if heat-treatment can eliminate contamination of surface traps when using BaCl₂ ablation targets. We present scanning electron microscope (SEM) and energy dispersive x-ray spectroscopy (EDS) images of the targets after ablation in Fig. 8. Neutral fluorescence is collected from all ablation targets in the same manner described in the manuscript, with a total of 48 spots being ablated (16 for each target). We find that melting $> 100 \mu\text{g}$ of BaCl₂ on platinum substrates produces uniform abla-

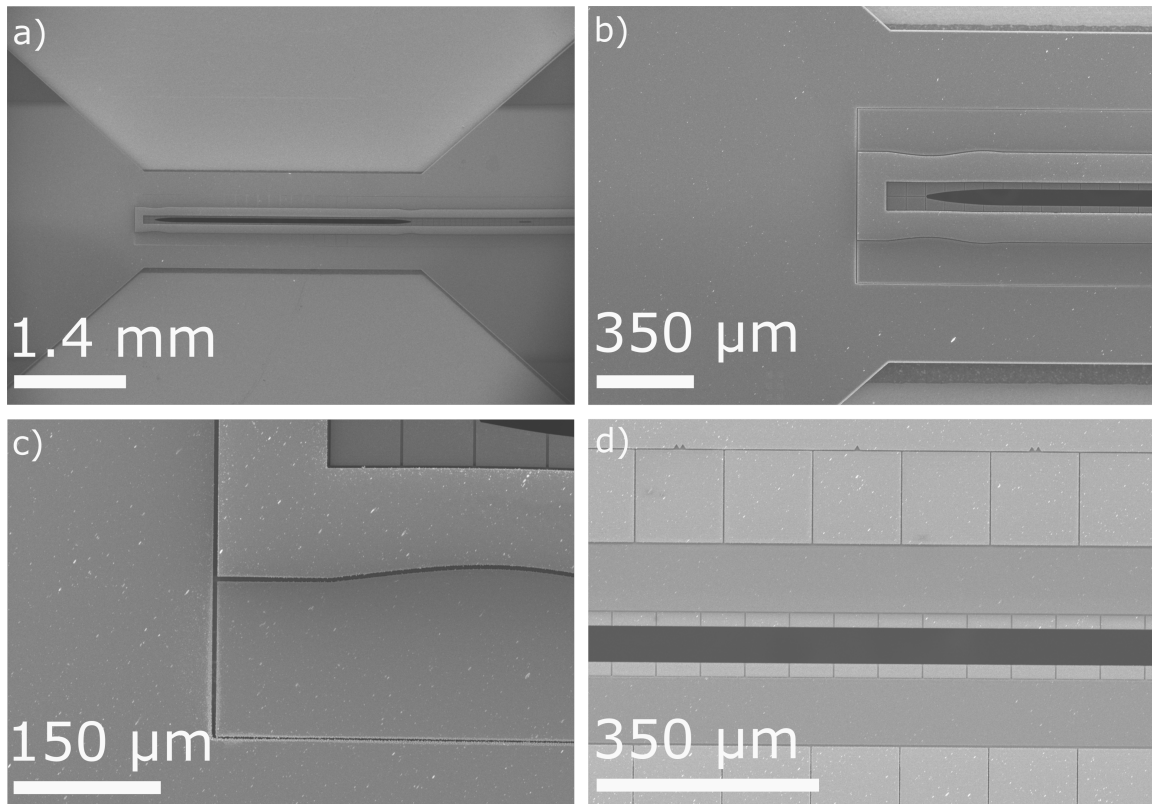


FIG. 6: a-d) SEM images of the test trap with large white BaCl₂ crystals visible from afar, as well as smaller crystals on outer and inner DC electrodes. The BaCl₂ crystal contamination is directional, but the sheer number of crystals on the surface is evident. The individual BaCl₂ crystal sizes usually range from 1 – 10 μm in length. We estimate this contamination is after > 50,000 ablation pulses using a similar ablation fluence to that as stated in the manuscript.

tion targets with spots that last > 1000 pulses, but that contamination of a surface trap would likely still occur as evident in Fig. 7.

We ablate heat-treated platinum targets with ~ 200 μg, 2 mg, and > 20 mg of BaCl₂. The deposition and heat-treatment follows the recipe outlined in the manuscript for these specific target types. The ablation targets are installed in the high-vacuum test chamber along with microfabricated gold chips from Angstrom Engineering Inc. (QA05-00180). The chips are ~ 25 mm away from the ablation targets in order to re-create a similar situation with a microfabricated surface trap. After ablation, the gold chips are removed and imaged as shown in Fig. 7.

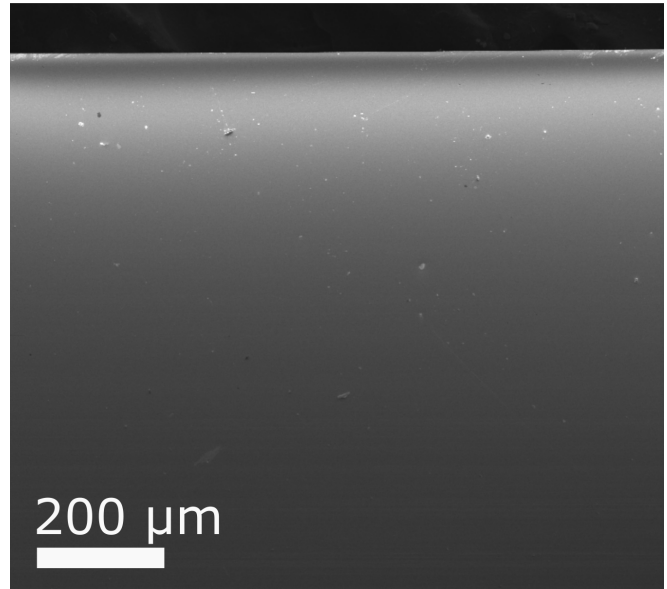


FIG. 7: SEM image of a gold prefabricated chip with BaCl₂ collected on the surface after ablation of macroscopic targets. This is from a ~ 200 μg BaCl₂ ablation target, proving that even after heat-treatment that small crystals can be ejected from the target without sublimation.

¹C. Monroe, R. Raussendorf, A. Ruthven, K. R. Brown, P. Maunz, L.-M. Duan, and J. Kim, *Phys. Rev. A* **89**, 022317 (2014).

²D. Kielpinski, C. Monroe, and D. Wineland, *Nature* **417**, 709 (2002).

³C. J. Ballance, T. P. Harty, N. M. Linke, M. A. Sepiol, and D. M. Lucas, *Phys. Rev. Lett.* **117**, 060504 (2016).

⁴M. J. Boguslawski, Z. J. Wall, S. R. Vizvary, I. D. Moore, M. Bareian, D. T. C. Allcock, D. J. Wineland, E. R. Hudson, and W. C. Campbell, *Phys. Rev. Lett.* **131**, 063001 (2023).

⁵P. Wang, C.-Y. Luan, M. Qiao, M. Um, J. Zhang, Y. Wang, X. Yuan, M. Gu, J. Zhang, and K. Kim, *Nature Communications* **12**, 233 (2021).

⁶F. A. An, A. Ransford, A. Schaffer, L. R. Sletten, J. Gaebler, J. Hostetter, and G. Vittorini, *Phys. Rev. Lett.* **129**, 130501 (2022).

⁷J. E. Christensen, D. Hucul, W. C. Campbell, and E. R. Hudson, *npj Quantum Information* **6**, 35 (2020).

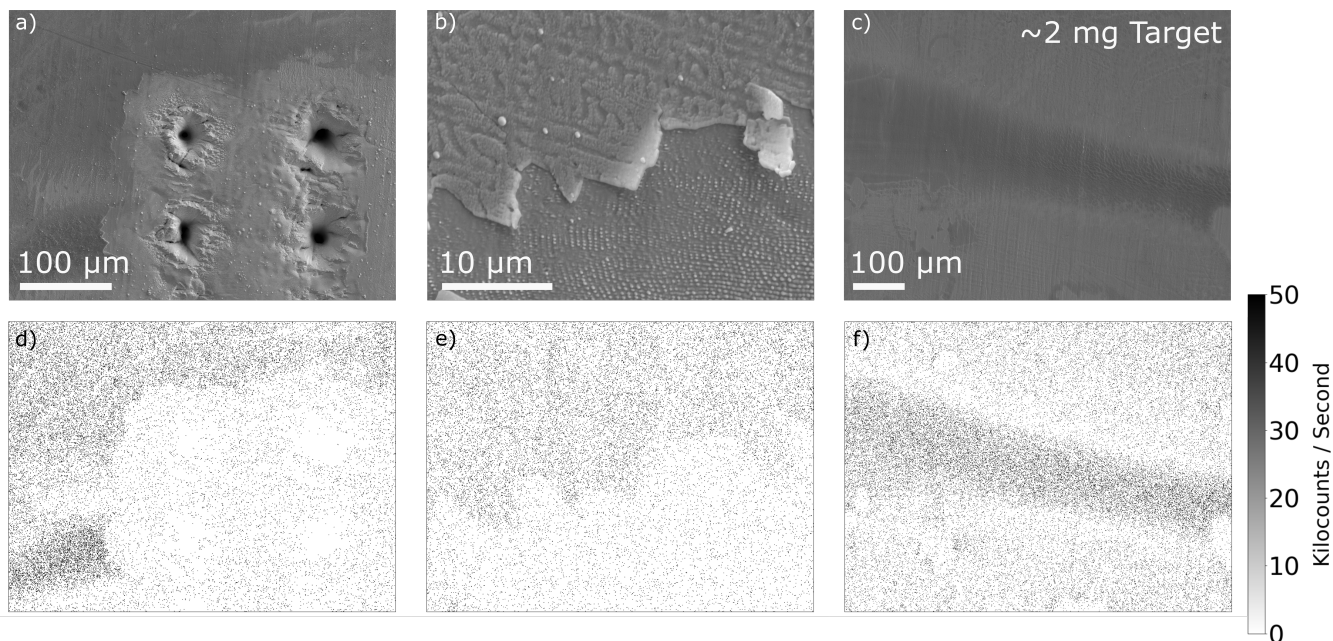


FIG. 8: a-c) SEM images of the heat-treated platinum ablation targets with ~ 2 mg of BaCl₂ deposited on the substrate. Note that a layer of BaCl₂ is formed as a crust on the surface of the platinum, making the ablation of these targets more consistent. The crust is removed after ablation. The size of the platinum strip is similar to the strip in Fig. 5b.

- ⁸D. Hucul, J. E. Christensen, E. R. Hudson, and W. C. Campbell, *Phys. Rev. Lett.* **119**, 100501 (2017).
- ⁹A. Binai-Motlagh, M. L. Day, N. Videnov, N. Greenberg, C. Senko, and R. Islam, *Quantum Science and Technology* **8**, 045012 (2023).
- ¹⁰P. J. Low, B. White, and C. Senko, “Control and readout of a 13-level trapped ion qubit,” (2023), arXiv:2306.03340 [quant-ph].
- ¹¹S. R. Vizvary, Z. J. Wall, M. J. Boguslawski, M. Bareian, A. Derevianko, W. C. Campbell, and E. R. Hudson, “Eliminating qubit type cross-talk in the *omg* protocol,” (2023), arXiv:2310.10905 [quant-ph].
- ¹²“Nuclear substances and radiation devices regulations,” (2015).
- ¹³Christensen, Justin E., “High-fidelity operation of a radioactive trapped ion qubit, ¹³³ba⁺,” (2020).
- ¹⁴B. M. White, P. J. Low, Y. de Sereville, M. L. Day, N. Greenberg, R. Rademacher, and C. Senko, *Phys. Rev. A* **105**, 033102 (2022).
- ¹⁵X. Shi, S. L. Todaro, G. L. Mintzer, C. D. Bruzewicz, J. Chiaverini, and I. L. Chuang, *Applied Physics Letters* **122**, 264002 (2023), https://pubs.aip.org/aip/apl/article-pdf/doi/10.1063/5.0149778/18024081/264002_1_5.0149778.pdf.
- ¹⁶Z. S. et al, in *51st Annual Meeting of the APS Division of Atomic, Molecular and Optical Physics*, Vol. 65, APS (American Physical Society, Portland, Oregon, 2020).
- ¹⁷A. V. B. et al, in *53rd Annual Meeting of the APS Division of Atomic, Molecular and Optical Physics*, Vol. 67, APS (American Physical Society, Orlando, Florida, 2022).
- ¹⁸N. Greenberg, B. M. White, P. J. Low, and C. Senko, “Trapping Ba⁺ with seven-fold enhanced efficiency utilizing an autoionizing resonance,” (2023), arXiv:2307.07627 [quant-ph].
- ¹⁹M. Rey, J. Walter, J. Harrer, C. M. Perez, S. Chiera, S. Nair, M. Ickler, A. Fuchs, M. Michaud, M. J. Uttinger, A. B. Schofield, J. H. J. Thijssen, M. Distaso, W. Peukert, and N. Vogel, *Nature Communications* **13**, 2840 (2022).
- ²⁰S. Das, A. Dey, G. Reddy, and D. D. Sarma, *The Journal of Physical Chemistry Letters* **8**, 4704 (2017), pMID: 28885853, <https://doi.org/10.1021/acs.jpclett.7b01814>.
- ²¹M. J. Hertaeg, C. Rees-Zimmerman, R. F. Tabor, A. F. Routh, and G. Garnier, *Journal of Colloid and Interface Science* **591**, 52 (2021).
- ²²F. Rösch, *Nuclear- and Radiochemistry* (De Gruyter, 2014).
- ²³<https://pubchem.ncbi.nlm.nih.gov/compound/Barium-133>, accessed: 2023-11-8.
- ²⁴J. I. Goldstein, D. E. Newbury, J. R. Michael, N. W. Ritchie, J. H. J. Scott, and D. C. Joy, *Scanning Electron Microscopy and X-Ray Microanalysis*, 4th ed. (Springer New York, NY, 2017).
- ²⁵M. C. Revelle, “Phoenix and peregrine ion traps,” (2020), arXiv:2009.02398 [physics.app-ph].
- ²⁶Q. A. Turchette, Kielpinski, B. E. King, D. Leibfried, D. M. Meekhof, C. J. Myatt, M. A. Rowe, C. A. Sackett, C. S. Wood, W. M. Itano, C. Monroe, and D. J. Wineland, *Phys. Rev. A* **61**, 063418 (2000).
- ²⁷L. Deslauriers, S. Olmschenk, D. Stick, W. K. Hensinger, J. Sterk, and C. Monroe, *Phys. Rev. Lett.* **97**, 103007 (2006).
- ²⁸J. A. Sedlacek, A. Greene, J. Stuart, R. McConnell, C. D. Bruzewicz, J. M. Sage, and J. Chiaverini, *Phys. Rev. A* **97**, 020302 (2018).